Microbial fuel cells with highly active aerobic biocathodes

Journal of Power Sources 324 (2016) 8–16

Contents lists available at ScienceDirect

Journal of Power Sources

journal homepage: www.elsevier.com/locate/jpowsour

Microbial fuel cells with highly active aerobic biocathodes

Edward M. Milner [a], Dorin Popescu [a], Tom Curtis [b], Ian M. Head [b], Keith Scott [a], Eileen H. Yu [a, *]

[a] Chemical Engineering and Advanced Materials, Newcastle University, Newcastle upon Tyne, NE1 7RU, UK
[b] Civil Engineering and Geosciences, Newcastle University, Newcastle upon Tyne, NE1 7RU, UK

HIGHLIGHTS

- Uncultured *Gammaproteobacteria* dominate in high-performing aerobic biocathodes.
- Microbial fuel cell biocathode performance comparable to a platinized cathode.
- Oxygen reduction catalysis linked to a bacterial electron transport chain.
- Additional electron transport pathways may be present at different poised-potential.

ARTICLE INFO

Article history:
Received 14 March 2016
Received in revised form
11 May 2016
Accepted 13 May 2016
Available online 21 May 2016

Keywords:
Aerobic biocathode
Microbial fuel cell
Uncultured *Gammaproteobacteria*
Poised-potential half-cell
Oxygen reduction reaction

ABSTRACT

Microbial fuel cells (MFCs), which convert organic waste to electricity, could be used to make the wastewater infrastructure more energy efficient and sustainable. However, platinum and other non-platinum chemical catalysts used for the oxygen reduction reaction (ORR) at the cathode of MFCs are unsustainable due to their high cost and long-term degradation. Aerobic biocathodes, which use microorganisms as the biocatalysts for cathode ORR, are a good alternative to chemical catalysts. In the current work, high-performing aerobic biocathodes with an onset potential for the ORR of +0.4 V vs. Ag/AgCl were enriched from activated sludge in electrochemical half-cells poised at −0.1 and + 0.2 V vs. Ag/AgCl. *Gammaproteobacteria,* distantly related to any known cultivated gammaproteobacterial lineage, were identified as dominant in these working electrode biofilms (23.3–44.3% of reads in 16S rRNA gene Ion Torrent libraries), and were in very low abundance in non-polarised control working electrode biofilms (0.5–0.7%). These *Gammaproteobacteria* were therefore most likely responsible for the high activity of biologically catalysed ORR. In MFC tests, a high-performing aerobic biocathode increased peak power 9-fold from 7 to 62 μW cm^{-2} in comparison to an unmodified carbon cathode, which was similar to peak power with a platinum-doped cathode at 70 μW cm^{-2}.

1. Introduction

Microbial Fuel Cells (MFCs) are a sustainable energy technology in which biodegradable organic chemicals are converted into electricity using bacteria, and provide a route for the efficient conversion of organic substrates present in wastewater directly into electricity. Given that wastewater treatment is the fourth largest user of energy in the UK, accounting for 1% of total energy consumption in England and Wales [1], renewable energy technologies which produce energy from wastewater, such as MFCs, may help to make the wastewater treatment infrastructure more energy efficient and sustainable.

MFCs work by coupling the anaerobic oxidation of organic matter by bacteria at the anode with the reduction of oxygen (most commonly) at the cathode, with electrons flowing through the external circuit and protons moving through solution or across a membrane separator, generating electrical power [2,3]. If MFC technology is to be adopted, then capital and operational costs must be lowered. Many of the biggest capital costs in the MFC system arise from the membrane and cathode. At the cathode, the oxygen reduction reaction (ORR) occurs;

$$O_2 + 4H^+ + 4e^- \rightarrow 2H_2O$$

* Corresponding author.
E-mail address: eileen.yu@ncl.ac.uk (E.H. Yu).

http://dx.doi.org/10.1016/j.jpowsour.2016.05.055

This reaction can be catalysed by chemically treated and untreated carbon materials [4–6], noble catalysts such as Pt, non-noble transition metal macrocycle catalysts such as cobalt tetramethoxyphenylporphyrin (CoTMPP) and iron phthalocyanine (FePc) [4,7,8], and by metal oxide catalysts, such as MnO_2 [4], as well as composite catalysts [9]. However, these chemical catalysts have associated costs, stability and sustainability issues. Activated carbons have been reported with comparable performance to Pt-doped carbon cathodes [10]. However, a major disadvantage of using carbon as an ORR catalyst is that the ORR occurs via a 2-electron mechanism producing hydrogen peroxide, which is undesirable for biological systems, and degrades fuel cell components including carbon corrosion [11]. Additionally, it has been found that clogging of the activated carbon microporous structure can lead to a reduction in MFC performance by 22–40% after one year of operation [12].

Mixed-community aerobic biocathode biofilms catalysing the ORR are a good substitute for chemical catalysts at the cathode, being free of cost, robust and sustainable. Several studies have reported using aerobic biocathodes, and a wide range of bacterial species belonging to the *Alphaproteobacteria* [13–16], *Betaproteobacteria* [14,16–21], *Gammproteobacteria* [13,14,16,18,19,22–28], *Bacteroidetes* [15,17,18,20,28,29] and other less well-known groups [14,15,30,31], have been identified as dominant in mixed-community aerobic biocathodes with onset potentials (E_{onset}) for ORR ranging from +0.40 to −0.15 V vs Ag/AgCl. Table 1 summarises various microorganisms reported as dominant in mixed-community aerobic biocathodes.

Variations in aerobic biocathode performance indicate that the biological mechanisms of ORR catalysis are different. Little is understood about these mechanisms of ORR catalysis, and what their biological function is [32,33].

The best performing aerobic biocathodes have the highest onset potential (E_{onset}) for ORR of around +0.4 V vs. Ag/AgCl, and have been developed in half-cells [22,34,35] and sediment MFCs [24,25]. In terms of community analysis, 49% of the clones recovered from the biocathode of a sediment MFC from an ocean cold seep were identified as *Pseudomonas fluourescens* [24], whilst DGGE of the carbon felt biocathode of a fresh water sediment MFC revealed a strong band classified as an uncultured *Proteobacteria* (97% certainty, 86% certainty for *Gammaproteobacteria*), which was not present in an equivalent closed circuit sediment MFC [25]. The sequences recovered from the fresh water sediment MFC were found to be 100% identical to *Gammaproteobacteria* clones recovered from steel plant waste [36]. Recently, Rothballer et al. identified similar uncultured *Gammaproteobacteria* as dominant (60.7% of 16S rRNA gene sequences in 454 pyrosequencer libraries) in a biocathode biofilm with an E_{onset} of +0.4 V cultivated on a graphite plate electrode [22].

Aerobic biocathode performances vary considerably in the literature, and a wide variety of different bacteria have been detected in these aerobic biocathodes. The objectives of this work were therefore to develop aerobic biocathode biofilms with high ORR activity, to identify the bacteria likely responsible for this ORR activity, and finally to assess the effect of these aerobic biocathodes on MFC performance in comparison to a typical MFC platinum cathode. This work is essential for designing better-performing aerobic biocathode biofilms for MFCs. Aerobic biocathode biofilms were first cultivated in electrochemical half-cells poised at −0.1 and +0.2 V to obtain high-performing aerobic biocathodes. These biocathodes were then assessed using a combination of turnover/non-turnover CV and CV in the presence of azide in order to link electrochemical features to physiological and mechanistic processes occurring at the electrode surface. The bacterial communities on these electrodes and on non-polarised controls were then analysed by Ion Torrent 16S rRNA gene sequencing in order to identify likely electroactive bacteria. MFC polarisations were conducted with dual chamber cells, with acetate fed bioanodes and an aerobic biocathode, Pt/C cathode and a plain carbon cathode.

2. Materials and methods

2.1. Setup of aerobic biocathode half-cells

A 3-electrode half-cell with a working electrode (WE), counter electrode (CE) and reference electrode (RE) was used to grow

Table 1
Dominant bacteria recovered from aerobic biocathodes ranked according to the onset potential for ORR. The bacteria have been identified to different taxonomic levels; phylum (p), class (c), order (o), family (f) and genus (g). The method of community analysis is given for each study; pyrosequencing (PS), clone libraries (CL), denaturing gel electrophoresis (DGGE) and illumina dye sequencing (IDS). Biocathode support materials used in each of these studies are carbon felt (CF), carbon cloth (CC), graphite plate (GP), graphite granules (GG) and carbon brush (CB). The type of BES using in each study is given; microbial fuel cell (MFC), sediment microbial fuel cell (SMFC), microbial solar cell (MSC) and half-cell (HC).

Type of BES	Support material	E_{ORR}(V)	Dominant bacteria in mixed community aerobic biocathodes	Method	Ref.
HC	GP	0.40	*Gammaproteobacteria (c)*	PS	[22]
MFC	CC	0.40	*Xanthomonadaceae (f), Xanthomonas (g)*	CL	[23]
SMFC	GP	0.40	*Pseudomonas (g)*	CL	[24]
SMFC	CF	0.40	*Gammaproteobacteria (c)*	DGGE	[25]
MFC	CF	0.25	*Pseudomonas (g), Rhodobacteraceae (f), Sphingomonadaceae (f)*	CL	[13]
MSC	GP	0.25	*Marinobacter (g)*	CL	[26]
HC	GP	0.25	*Chromatiaceae (f)*	IDS	[27]
HC	CP	0.25	*Bacteroidetes (p)*	CL	[29]
MFC	CB	0.20	*Nitrospira (g), Nitrosomonas (g), Nitrobacter (g), Alkalilimncola (g)*	CL	[14]
MFC	CC	0.20	*Rhizobiales (o), Phycisphaerales (o), Planctomycetales (o), Sphingobacteriales (o)*	PS	[15]
MFC	GG	0.15[a]	*Azovibrio (g), Bacteroidetes (p)*	CL	[17]
MFC	GG	0.15[a]	*Xanthomonas (g), Bacteroidetes (p)*	CL	[28]
HC	CC	0.00	*Deinococcus-Thermus (p), Gemmatimonadetes (p)*	PS	[30]
MFC	CF	−0.10	*Acinetobacter (g), Sphingobacterium (g), Acidovorax (g)*	CL	[18]
MFC	CC	−0.15	*Chloroflexus (g)*	PS	[31]
MFC	CF	–	*Betaproteobacteria (c), Gammaproteobacteria (c)*	PS	[19]
MFC	Various	–	*Comamonas (g), Sphingomonas (g), Acidovorax (g)*	CL	[20]
MFC	CB	–	*Achromobacter (g)*	PS	[21]
MFC	CB/GG	–	*Gammaproteobacteria (c), Agrobacterium (g), Achromobacter (g)*	DGGE	[16]

[a] Redox peak mid-point potential.

individual aerobic biocathode biofilms. The WE was a rectangular piece of carbon felt with an area of 12.2 cm^2 (19 × 64 mm) and a thickness of 5 mm (VWR, Cat. No. 43200.RR, Alfa Aesar). The carbon felt was acetone-washed beforehand and held between a polytetrafluoroethylene (PTFE) window and backing plate using PTFE bolts, exposing only one side of the carbon felt to the electrolyte. A graphite plate was used to make contact between the carbon felt and the external circuit. The CE was a rectangular 35 cm^2 piece of Pt mesh attached to a titanium wire, and the RE was an Ag/AgCl electrode (BASi, RE-5B) housed within a polypropylene luggin capillary containing a 3 M NaCl agar salt bridge (0.208 V vs SHE). The tip of the luggin capillary was less than 5 mm from the working electrode to ensure a small ohmic resistance. The half-cell setup is provided as a diagram in Supplementary material. The potentials in this paper are against the Ag/AgCl reference electrode, unless otherwise stated.

2.2. Inoculation and operation of aerobic biocathode half-cells

All aerobic biocathodes discussed in this work were grown in poised-potential half-cells and were operated in under the same conditions. Each half-cell contained 1 L of minimal medium containing phosphate buffer (50 mM, pH 5.8) and trace nutrients for the bacteria. A pH of 5.8 was chosen to increase the reduction potential for O_2 to +0.67 (pO_2 = 0.2 atm) and therefore the bacterial energy gain from the electrode, whilst also maintaining the buffer capacity of the medium. The trace nutrients were 10 ml L^{-1} of a macro nutrient solution, 1 ml L^{-1} of a micro nutrient solution, and 1 ml L^{-1} of a vitamin solution, as described by Heijne et al. [37,38], with a few minor changes. Details of these solutions can be found in the Supplementary material.

Aerobic biocathode half-cells were inoculated with one of two different inocula and operated at one of two different poised-potentials. The inoculum used was either 10% (v/v) of activated sludge, or 100% (v/v) of the effluent from an operating half-cell with an aerobic biocathode. The activated sludge was obtained from Tudhoe wastewater treatment plant in the North East of England. Activated sludge was chosen as the primary inoculum for the half-cells as it has been previously used successfully to generate aerobic biocathodes with E_{onset}(ORR) values of +0.4 V [34,35], and it is known to be a source of a diverse range of bacteria [39]. The poised-potentials used were either −0.1 and + 0.2 V, or without poised-potential for the control cells. The most negative poised-potential chosen for biocathode formation on carbon felt was −0.1 V, to avoid abiotic formation of peroxide through 2-electron ORR on carbon, and to maximise the potential energy gain for the bacteria. +0.2 V was selected as a poised-potential as it is half-way between −0.1 V and the E_{onset}(ORR) for high-performing aerobic biocathodes of +0.4 V. Combinations of inoculum and poised-potential gave 4 different treatments; activated sludge-inoculated half-cells poised at −0.1 V, half-cell effluent-inoculated half-cells poised at −0.1 V, half-cell effluent-inoculated half-cells poised at +0.2 V, and half-cell effluent-inoculated half-cells which were not polarised. Duplicate half-cells were operated for each treatment, giving a total of eight half-cells. The half-cells operated in this study are summarised in Table 2.

The half-cells were operated in batch mode. The working electrode potential was applied using a potentiostat (Sycopel, UK), and I (A) measured continuously with one day intervals. In all of the half-cells, air was sparged into the half-cell chamber using an air pump and air sparger to maintain the dissolved oxygen at levels above 7.0 mg L^{-1}. The temperature for all half-cells was maintained at 30 °C throughout. All polarised half-cells were operated for at least 1 month after initial enrichment, whilst the two unpolarised half-cells were operated for 1 month. Additional details regarding half-cell operation can be found in Supplementary material.

Table 2
Table giving the inoculum and poised-potential used for the half-cells in the study. All half-cells were operated in duplicate, giving a total of 8 half-cells.

Inoculum	Poised-potential (V vs Ag/AgCl)
Activated sludge	−0.1
Half-cell effluent	−0.1
Half-cell effluent	+0.2
Half-cell effluent	Non-polarised

2.3. Electrochemical analysis

The WE of the half-cells was characterised periodically by CV using an Autolab PGSTAT302 potentiostat (Metrohm, Switzerland). CVs were recorded over a scan range from +0.5 V to −0.2 V, using a scan rate of 5 mV s^{-1}, and the last scan of 4 was taken as the stabilised CV response. CVs were recorded in the absence of O_2 for some of the half-cells. O_2 was removed from the half-cells by sparging the with N_2 and polarising the electrode at the same potential as used for enrichment for one hour and until the reduction current was > −100 μA, then a N_2 blanket was maintained on the solution surface throughout the electrochemical characterization. CV in the presence of azide were carried out at the end of the operational period for some of the half-cells by adding 1 ml L^{-1} of a 2% (v/v) NaN_3 stock solution (0.3 mM final concentration) followed by stirring of the electrolyte for 1 min using a magnetic stirrer before taking the CV.

2.4. Microbial community analysis

Microbial community analysis was carried out on electrode samples. PCR amplified 16S rRNA gene fragments from the microbial community on the electrode were sequenced using ion semiconductor sequencing technology targeting the V4–V5 hypervariable region of the 16S rRNA gene of bacteria and archaea (481 base pairs). A small piece of electrode weighing ca. 0.25 g was cut from the carbon felt electrode and the DNA extracted using a DNA isolation kit (MO BIO, USA). PCR was carried out on the extracted DNA using a barcoded V4f primer and a non-barcoded V5r primer, with the PCR reagents provided from a kit following the manufacturer's instructions (MegaMix-Blue, Cambio, UK). Following initial denaturation at 94 °C for 4 min, 30 cycles of PCR were carried out using a thermal cycler (Techne TC-512 Thermal Cycler, Bibby Scientific, Staffordshire, UK) with the following program; 94 °C for 30s, 56 °C for 30s, 72 °C for 45s. At the end of the 30 cycles, the temperature was held at 72 °C for 7 min. The resulting PCR products were purified by two rounds of purification using AMPure XP magnetic bead purification, following the manufacturer's protocol (Beckman Coulter, USA). Purified PCR products were quantified using a Qubit fluorometer (Life Technologies, USA). The purified PCR products were then pooled and diluted to 26 pM. Template preparation was then carried out on the pooled sample using the Ion OneTouch (Life Technologies, USA) procedure before sequencing using an Ion Torrent Personal Genome Machine (Life technologies, USA).

The resulting community 16S rRNA gene sequence data were processed using QIIME [40]. The sequences were clustered into OTUs at 97% sequence identity, corresponding to species-level discrimination using the UCLUST clustering method. Representative sequences from each OTU were determined based on the most abundant sequences in each OTU and their taxonomic affiliation was assigned using the Greengenes database. An OTU table was built based on the assigned taxonomy and number of times an OTU

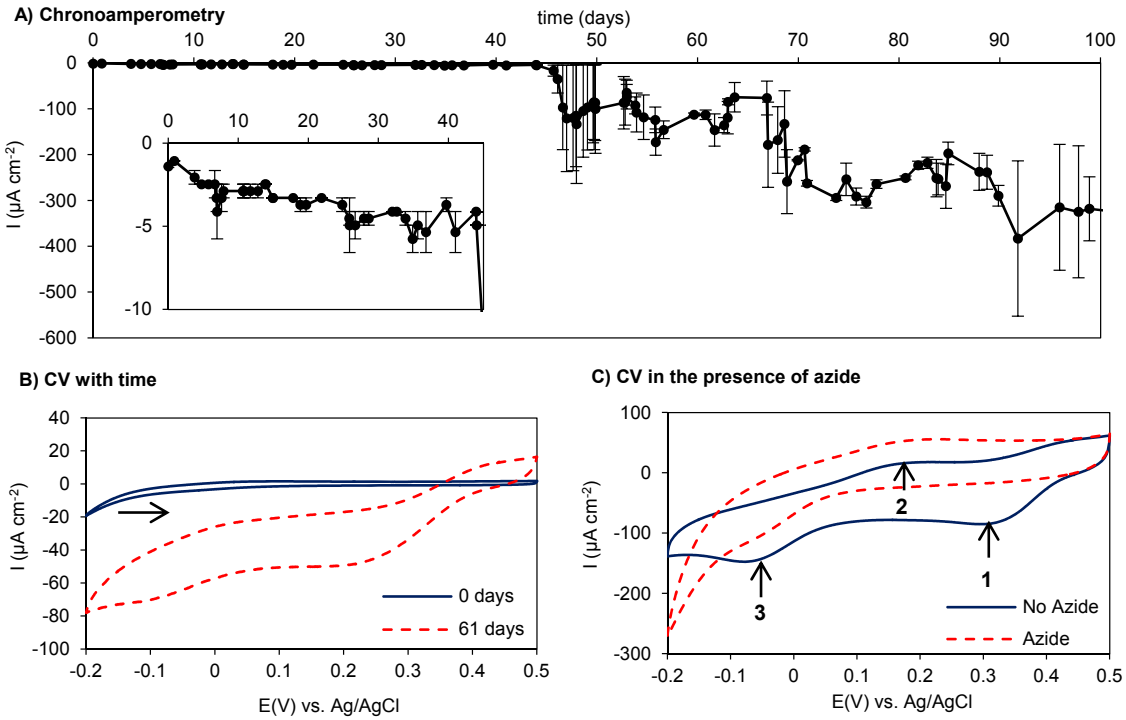

Fig. 1. Biofilm growth; (A) chronoamperometry for duplicate half-cells poised at −0.1 V and inoculated from activated sludge (error bars are the range), (B) CV in the presence of oxygen at 0 and 61 days for the first duplicate half-cell, and (C) CV in the presence of oxygen and azide recorded at the end of the operational period for the first duplicate half-cell. Equivalent CV to B and C for the second duplicate half-cell can be found in Supplementary material as Fig. S3.

appeared in each sample. The sequences were then aligned using the PyNast algorithm to a pre-aligned database of template sequences from the Greengenes database, the alignment was filtered, and chimeric sequences were identified using the ChimeraSlayer algorithm and removed. The OTUs were plotted graphically according to taxonomic assignment, and a beta diversity distance matrix was calculated using weighted UniFrac for all samples in the study. This was analysed using principal coordinates analysis. A phylogenetic tree containing only *Gammaproteobacteria* was calculated using FastTree [41], and using 16S rRNA sequence data obtained from the present study and from GenBank. Representative sequences for the four most abundant uncultured Gammaproteobacteria OTUs from this study (denovo3034, denovo4677, denovo5 and denovo6950) were deposited in GenBank. They are accessible in GenBank under accession numbers KX230045, KX230046, KX230047 and KX230048.

2.5. MFC polarisations using dual chamber MFCs

The Pt cathode of an existing dual chamber glass MFC was replaced with an aerobic biocathode grown in a poised-potential half-cell (secondary inoculum, −0.1 V poised-potential), with an area of 12 cm^2. The setup for this MFC is given in the Supplementary material for this article. The biocathode was cultivated as described previously and connected to a gold plated titanium wire. The bioanode used carbon felt support, with the area of 33 cm^2, and was connected via a 316 stainless steel rod. Ag/AgCl reference electrodes were inserted into both bioanode and biocathode chambers to measure the anode and cathode potentials respectively. The same minimal medium as in the half-cells was used in the cathode chamber of the MFC, with the exception that 50 mM of pH 7.0 phosphate buffer was used instead of pH 5.8 phosphate buffer. The bioanode used the same minimal medium as at the biocathode, but with the addition of 1.0 g L^{-1} of sodium acetate. Polarisation curves were recorded by varying the external resistance from high to low values in 20 min intervals (open circuit, then 534,000 Ω–52 Ω), whilst recording the cell voltage, cathode potential and anode potential simultaneously. In order to assess the improvement in MFC performance that an aerobic biocathode biofilm makes, the same MFC was tested with a plain carbon felt electrode with no biocathode biofilm. Additionally, a carbon paper electrode of the same geometric area coated with Pt/C ink containing Pt at 0.57 mg cm^{-2} loading was also tested. The Pt ink contained Pt/C (20% Pt by weight, Alfa Aesar) and 10% Nafion binder (Nafion resin solution with 5% by weight Nafion, Sigma Aldrich), and was prepared and applied to the carbon paper electrode as described elsewhere [42].

3. Results and discussion

3.1. Electrochemical analysis

3.1.1. Aerobic biofilm growth

The average chronoamperometric (CA) current with time for the duplicate activated sludge inoculated aerobic biocathodes poised at −0.1 V was determined (Fig. 1). From 0 to 50 days, the average CA reduction current was less than 5 μA cm^{-2} (inset) and the open-circuit potential (OCP) less than 0.1 V. At 50 days, the reduction current increased to 204 ± 80 μA cm^{-2} and the OCP to 453 ± 14 mV for the rest of the operational period (Fig. 1). CV on the two half-cells at 61 days, after a considerable increase in CA reduction current and OCP for both half-cells, were markedly different in comparison to CV spectra taken at 0 days (Fig. 1B. Equivalent CV for the duplicate half-cell can be found in Supplementary material). This resulted from the appearance of an ORR wave with an onset potential value of +0.4 V, which is considerably more positive than the abiotic ORR wave at t = 0 days with an onset potential of approximately −0.1 V. The high onset potential of 0.4 V has been

observed previously in the literature, and is believed to be due to the activity of aerobic, electrotrophic bacteria [35], which are thought to gain energy for metabolism and growth by using electrons derived from the electrode to generate ATP and to fix CO_2 into biomass, simultaneously catalysing the ORR.

There were significant differences in enrichment times, depending on how the half-cells were inoculated. The half-cells inoculated from activated sludge took 47–56 days to enrich (CA reduction current > 100 μA cm^{-2}), which was significantly greater than the half-cells inoculated with effluent from an operating biocathode, which took between 3 and 9 days to enrich. This difference is due to inoculation from effluent enriched in electroactive bacteria in the case of the secondary inoculum half-cells, whilst enrichment from activated sludge takes a much longer period of time, as the electroactive bacteria are likely in much lower abundance from activated sludge. One theory for the long enrichment time from activated sludge is that the presumed autotrophs which are responsible for ORR catalysis in aerobic biocathodes are suppressed due to competitive heterotrophic microbial growth fed on the organic break down products from activated sludge decomposition.

3.1.2. Determining bacterial ORR activity using azide inhibitor

To determine if the ORR current observed in the CV was related to a putatively ATP-producing bacterial electron transport chain, the half cells were treated with sodium azide [43]. Azide inhibits cytochrome c oxidase, an enzyme which catalyses the reduction of oxygen to water in the electron transport chain of many aerobic bacteria. Aerobic bacteria which use the electrode as part of an electron transport chain to generate ATP should be inhibited when azide is added, and any associated ORR current should be significantly reduced. The electrochemical response of the primary inoculated half-cell polarised at −0.1 V to azide inhibition is shown in Fig. 1 (Equivalent CV for the duplicate half-cell is given in Supplementary material). The biologically catalysed ORR wave was removed on addition of sodium azide (Fig. 1C, feature 1) while the other redox peaks (Fig. 1C, oxidation peak – features 2, and reduction peak – feature 3) were less affected. This demonstrates that the ORR activity from the biocathode is linked with an oxygen-reducing bacterial electron transport chain. This CV behaviour was also apparent in the duplicate half-cell (see Supplementary material). Additionally, sodium azide is also known to specifically inhibit Gram negative bacteria [43–45], which indicates that the bacteria responsible for the ORR activity are likely to be Gram negative.

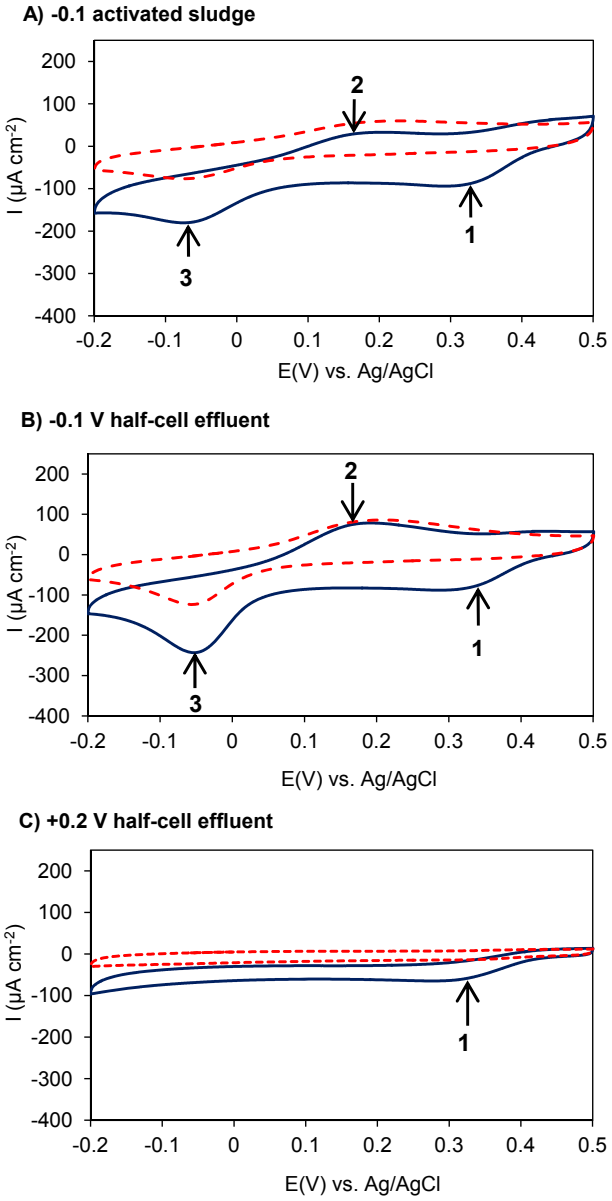

Fig. 2. CV (μ = 5 mV s^{-1}) recorded in the presence (solid lines) and absence (dashed lines) of oxygen for half-cells using different poised-potential and inoculum; (A) −0.1 V/activated sludge inoculum, (B) −0.1 V/half-cell effluent inoculum and (C) +0.2 V/half-cell effluent inoculum. Features 1: ORR wave, 2: oxidation peak, and 3: reduction peak. Equivalent CV to A, B and C for the duplicate half-cells can be found in Supplementary material as Fig. S4.

Table 3
Table showing the enrichment period and average CA current from all polarised half-cells in the study. Standard deviations are given for the average currents.

Half-cell	Chronoamperometry	
	Enrichment time days	I (average) μA cm^{-2}
Activated sludge inoculum, −0.1 V	56	−195 ± 95
Activated sludge inoculum, −0.1 V	47	−212 ± 64
Half-cell effluent inoculum, −0.1 V	3	−208 ± 42
Half-cell effluent inoculum, −0.1 V	5	−155 ± 56
Half-cell effluent inoculum, +0.2 V	9	−129 ± 37
Half-cell effluent inoculum, +0.2 V	7	−130 ± 66

3.1.3. Effects of poised-potential on bacterial electron transfer mechanisms

The average CA currents for the 6 polarised half-cells were similar, with no statistically significant changes between the three treatments (p = 0.097, ANOVA), regardless of inoculation or whether the poised-potential was −0.1 V or +0.2 V (Table 3). It has been reported previously that performance of aerobic biocathodes is greatest when they are poised at +0.15 V [35] and +0.28 V [34], however, no clear difference in performance was observed at the two potentials used in this study.

To elucidate details of the mechanism of electron transfer occurring at the electrode surface, CV were recorded in the presence and absence of O_2 at the end of the experimental period for

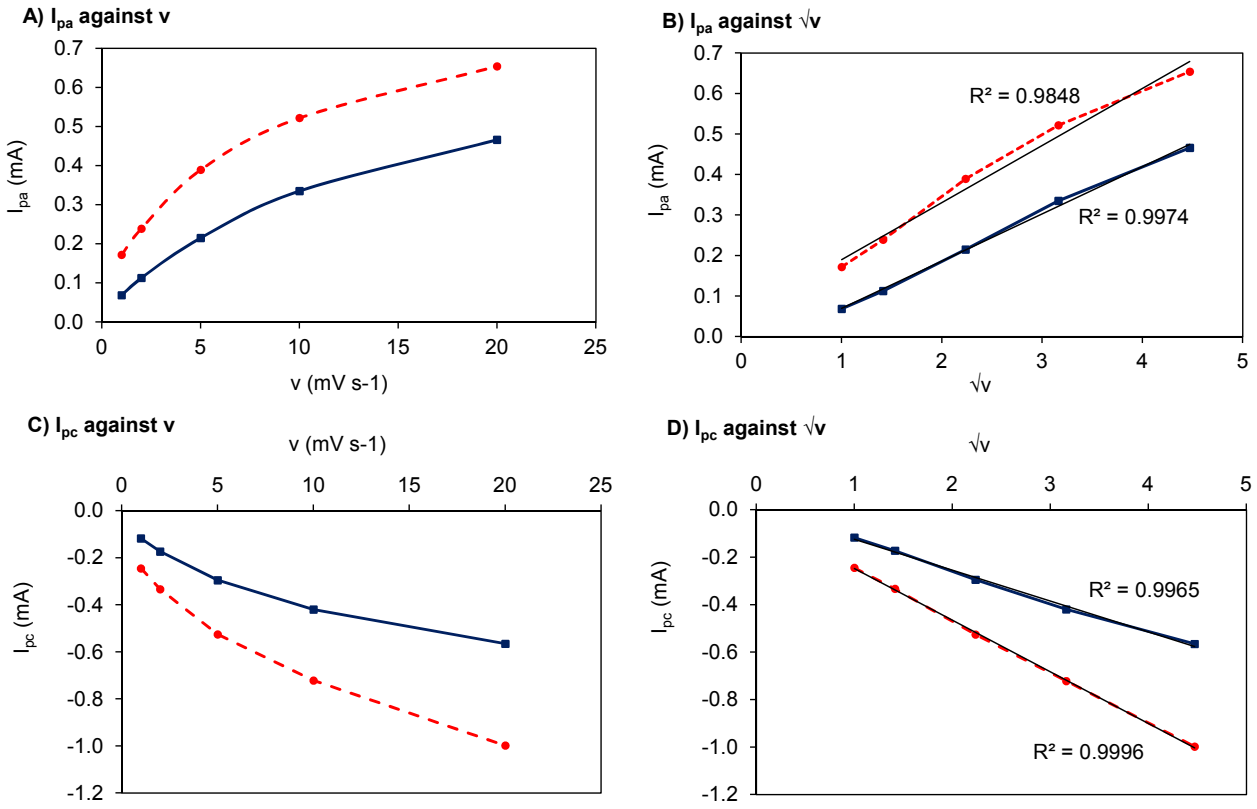

Fig. 3. Peak analysis of redox peaks identified in CV of the −0.1 V poised-potential half-cell inoculated from half-cell effluent; (A) I_{pa} against ν (B) I_{pa} against $\nu^{1/2}$, (C) I_{pc} against ν, and (D) I_{pc} against $\nu^{1/2}$ where ν is the scan rate in mV/s (1–25 mV s^{-1} range), I_{pa} is the anodic peak current and I_{pc} is the cathodic peak current.

the polarised half-cells (Fig. 2. Equivalent CV for the duplicate half-cells is given in Supplementary material as Fig. S4). Important electrochemical features have been labelled (1–3) in Fig. 2. Feature 1 is an ORR wave present under aerobic but not anaerobic conditions, whilst features 2 and 3 are an oxidation and reduction peak, respectively, which are present under both aerobic and anaerobic conditions.

In the spectra for all half-cells, the ORR wave (Fig. 2; feature 1) is removed by sparging under N_2. Further comparison of the CV under N_2 show how the half-cells polarised at −0.1 V still possess an oxidation peak at +0.2 V (Fig. 2; feature 2) and a reduction peak at −0.05 V (Fig. 2; feature 3) in their spectra, which form a reversible redox couple with a half wave potential ($E_{1/2}$) of +0.1 V. In the absence of O_2, this reversible redox peak must be associated with an electrochemical reaction which is not coupled with O_2 reduction. Therefore, the CV spectra show two distinct electrochemical processes (EPs), one which is almost certainly an electron transfer pathway coupled with oxygen reduction in a conventional ATP generating electron transport chain, EP1 (Figs. 1 and 2; feature 1), and a second reversible process, EP2 (Figs. 1 and 2; features 2 and 3), which may be a parallel electron transfer pathway or some other unknown surface reaction occurring within the biofilm which otherwise is not directly involved in oxygen reduction. Given that no peaks are observed in the non-turnover CV (i.e. in the absence of oxygen) near +0.4 V, EP1 likely relates to oxygen reduction, whereas if EP2 (Fig. 2, features 2 and 3) is an electron transfer pathway to the bacteria, it could potentially be due to a bacterially produced electron mediator or reversible oxidation of e.g. a cytochrome interacting with the electrode surface, leading to a reversible redox peak in the absence of O_2.

An important observation is that the aerobic biocathodes poised at −0.1 V possess both EP1 and EP2, whereas the aerobic biocathode poised at +0.2 V possesses only EP1. For EP2, the $E_{1/2}$ of +0.1 V for the redox couple means that it would be unable to accept electrons from a cathode poised at +0.2 V. This is consistent with the observation that EP2 was not detected in systems where the cathode was poised at this voltage. A cathode poised at +0.2 V could however donate electrons to a cell component with a more negative potential than the +0.4 V onset potential for the ORR observed (Fig. 2), and is therefore theoretically able to donate electrons to an ATP-generating electron transport chain between the electrode and O_2.

To see whether EP2 in cells poised at −0.1 V, was surface absorbed or diffusive, CV were recorded in the absence of O_2 at different scan rates (ν = 1–25 mV s^{-1}) for the duplicate half-cell effluent-inoculated half-cell poised at −0.1 V, and the oxidation and reduction peak heights were plotted against *ν* and *ν* (Fig. 3). Linearity was observed in the plots of peak height versus *ν*, which implies that the reversible peak is diffusive and suggests that the process is not confined to the surface of the electrode, and may be indicative that EP2 represents a mediated electron transfer (MET) process. However, there are other models which may also explain this behaviour. For example, it has been proposed that *Geobacter sulfurreducens* is able to use a network/chain of c-type cytochromes to shuttle electrons to the electrode surface [46]. Such a network may also produce a diffusive-like peak response in CV. The other model proposed for *Geobacter sulfurreducens* is electron shuttling via metallic-like nanowires from outer membrane cytochromes to the electrode surface [47]. MET was previously suggested as a potential mechanism of electron transfer for aerobic biocathodes by

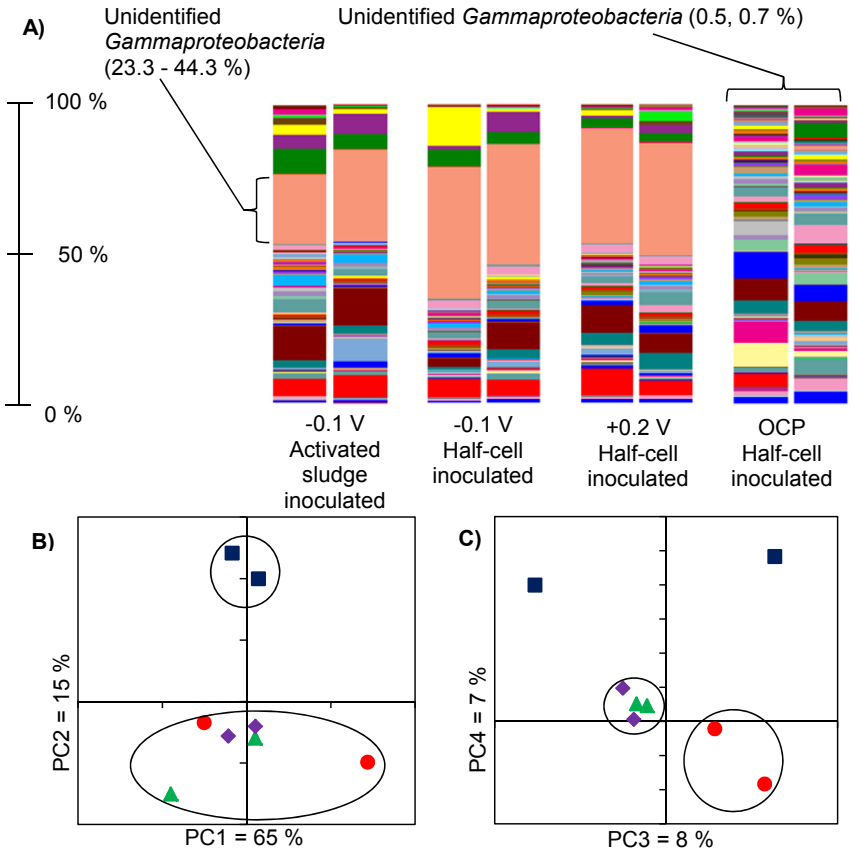

Fig. 4. Biofilm community analysis; (A) stacked bar charts showing percentage sequence abundance according to taxonomy at the genus level of the electrode biofilms and (B and C) comparison of microbial communities from different electrode biofilms using principal coordinate analysis based on weighted UniFrac similarity of the 16S rRNA gene profiles. −0.1 V activated sludge inoculum (red circles), −0.1 V half-cell effluent inoculum (green triangles), +0.2 V half-cell effluent inoculum (purple diamonds) and non-polarised half-cells inoculated with half-cell effluent (blue squares). (For interpretation of the references to colour in this figure caption, the reader is referred to the web version of this article.)

Freguia et al. [48]. The authors found an unidentified redox peak at −270 mV and a redox peak at +60 mV from pyrroloquinoline quinone (PQQ) in the non-turnover CV of a biofilm of *Acinetobacter calcoaceticus*. Addition of PQQ enhanced the catalytic current response, and it was suggested that *Acinetobacter calcoaceticus* was able to use this as an electron mediator to catalyse electron transfer from the electrode to the bacteria [48].

The energy available to the bacteria using electrons from an electrode can be calculated by considering the Gibbs free energy, given the following equation [49];

$$\Delta G^{0\prime} = -nF\Delta E^{0\prime}$$

where $\Delta E^{0\prime} = E^{0\prime}$ *(electron acceptor)* $- E^{0\prime}$ *(electron donor)*, n = 4 and F = 96.48 kJ mol^{-1}. Using the E_{onset} of +0.4 V (EP1) as the potential for the terminal oxidase cytochrome c oxidase, for biocathodes poised at +0.2 V, $\Delta E^{0\prime}$ = 0.40−0.20 = +0.20 V and $\Delta G^{0\prime} = -77$ kJ mol^{-1} of O_2, assuming electrons are accepted at the potential of the electrode. If EP2 also represents an electron transfer pathway which the bacteria are able to use to derive energy from the electrode, then $\Delta E^{0\prime}$ = 0.40−0.10 = +0.30 V (using the redox peak $E_{1/2}$ of +0.10 V as the electron donor potential) and $\Delta G^{0\prime} = -116$ kJ mol^{-1} of O_2. The energy used to form 1 mol of ATP from ADP is +30.5 kJ mol^{-1} of O_2 [49], therefore 3 molecules of ATP could potentially be generated by bacteria utilising 4 electrons from the electrode through EP2, or a maximum of 2 molecules of ATP when the electrode potential is +0.2 V.

This analysis demonstrates how the bacteria may adapt their electron transfer pathways to different cathode potentials in order to increase ATP yield. It has been shown previously that for *Geobacter sulfurreducens* bioanode biofilms fed acetate, the appearance of different redox peaks in their non-turnover CV is dependent on the potential at which they were cultivated, suggesting that the bacteria may regulate their use of different electron transfer pathways in response to different applied potential [50]. This may also be the case for aerobic biocathodes, but further electrochemical investigations are required.

3.2. Microbial community analysis of aerobic biocathodes with high ORR activity

The bacterial communities on the working electrodes of all six polarised half-cells and two unpolarised control half-cells were analysed (Fig. 4). The most striking difference between the polarised and unpolarised electrodes is the domination of the polarised electrodes by sequences recovered from *Gammaproteobacteria* belonging to a group not represented by any known cultured organisms. These accounted for 23.3–44.3% of the total sequences from the polarised electrodes, and only 0.5–0.7% for the unpolarised electrodes.

When comparing the communities explicitly through weighted beta diversity, 95% of the total diversity could be explained by the first four axes from the principal coordinates analysis, with 65% explained by the first axis, 15% explained by the second, 8% by the third and 7% by the fourth. For the first two axes, explaining 80% of the observed variation, the polarised half-cells clustered away from

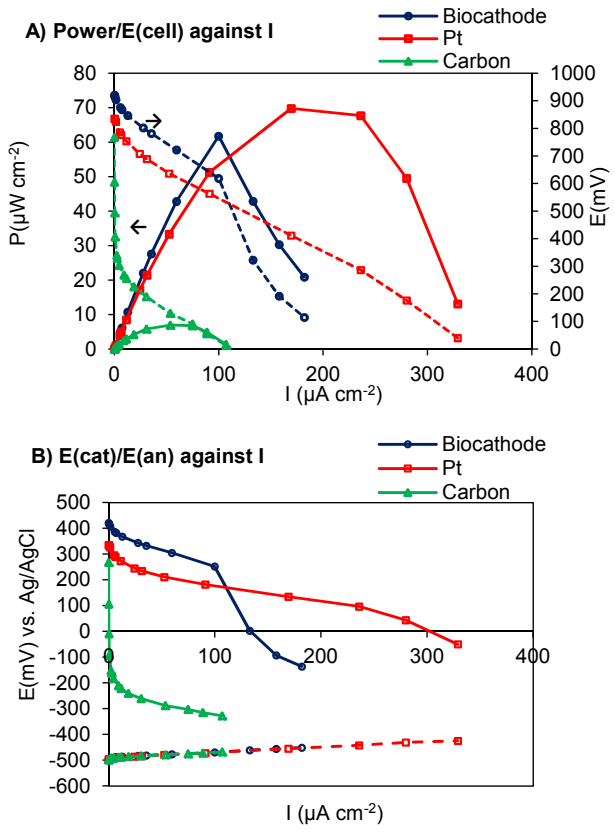

Fig. 5. Polarisation curves for an MFC using a biocathode cultivated on carbon felt, a Pt cathode, and a carbon felt cathode with no biofilm; (A) power density, (B) anode and cathode potential.

the non-polarised controls, showing that the polarised and non-polarised communities were distinct from one another. For the next 15% of community variation, the poised-potential half-cells remained clustered apart from the non-polarised communities. Additionally to this, the half-cell effluent inoculated half-cells poised at both −0.1 and +0.2 V clustered tightly together, and separately to the activated sludge inoculated half-cells poised −0.1 V, indicating that inoculum type influenced community composition more than poised-potential.

An OTU representing a group of uncultured *Gammaproteobacteria* dominated the communities of the polarised half-cells, and were in low abundance on the electrodes of non-polarised half-cells. Therefore, these bacteria are likely to play an important part in the biologically catalysed ORR. This would be consistent with the fall in ORR current on addition of azide, as azide selectively inhibits Gram-negative bacteria, such as *Gammaproteobacteria*, and not Gram-positive bacteria [43–45]. There was a lower percentage of reads associated with uncultured gammaproteobacterial OTUs for activated sludge inoculated half-cells poised at −0.1 V (23.3%, 30.6%) in comparison to the secondary inoculate half-cells (40.4%, 44.3%), which is consistent with these cells clustering away from the others more strongly in the comparative analysis (Fig. 4C).

Comparison of the uncultured *Gammaproteobacteria* identified in this study with named *Gammaproteobacteria* from various aerobic biocathode studies from the literature [13,20,22,24,26,29,36,48,51–54] was carried out by constructing a phylogenetic tree from 16S rRNA gene sequences from GenBank and recovered in this study (see Supplementary material). Representative sequences for the four most abundant uncultured *Gammaproteobacteria* OTUs from this study, denovo4677 (56%), denovo3034 (9%), denovo6950 (6%) and denovo5 (3%), were included in the phylogenetic analysis (abundances in brackets are relative to the number of sequences assigned as uncultured *Gammaproteobacteria*). They form a monophyletic clade (highlighted red in Fig. S5 of Supplementary material) with uncultured *Gammaproteobacteria* isolated from steel waste (EU447525.1, EU447521.1 and EU447526.1) [36] and those dominant on a graphite electrodes in the study by Rothballer et al. (KJ600342.1, KJ600388.1 and KJ600599.1) [22].

The uncultured *Gammaproteobacteria* which were found to be dominant on polarised electrodes in this study are likely responsible for the ORR activity of high-performing aerobic biocathodes with an ORR onset potential +0.4 V. Additionally, according to the phylogenetic analysis (Fig. S5 of Supplementary material), closely related bacteria have also been found to be dominant on other high-performing biocathodes from the literature.

3.3. MFC performance with an aerobic biocathode

Performance of an operational MFC with a plain carbon felt electrode, one with a biocathode biofilm, and a carbon paper electrode of the same geometric area with Pt loading of 0.57 mg cm^{-2} was compared with both the anolyte and catholyte buffered to pH 7.0 (Fig. 5). The MFC had a peak power density of 62 μW cm^{-2} when operated with a biocathode, 7 μW cm^{-2} when operated with a plain carbon felt electrode, and 70 μW cm^{-2} with a carbon paper electrode loaded with Pt.

In this MFC, enrichment of carbon felt with aerobic biocathode bacteria increased the peak power density of the MFC by almost an order of magnitude in comparison to plain carbon felt, and the biocathode gave 89% of the peak power density of the MFC with a Pt cathode. It can be observed from Fig. 5(b) that the potential of anodes of the MFCs were the same, whereas the cathode potential was different depending on which cathode was used. This indicates that the differences in power output of the MFCs are due to the different cathodes used. The use of an aerobic biocathode is a promising alternative to Pt cathodes. The performance of this aerobic biocathode MFC compared favourably with other aerobic biocathode MFCs from the recent aerobic biocathode MFC literature, with peak powers of 68 μW cm^{-2} [55], 110 μW cm^{-2} [14], 50 μW cm^{-2} [56] and 38 μW cm^{-2} [57].

4. Conclusions

Aerobic biocathode with an onset potential for the ORR of +0.4 V for ORR have been successfully developed. The poised-potentials applied during biofilm enrichment may affect the electron transfer mechanism. Community analysis shows that an uncultured group of *Gammaproteobacteria* dominated in the aerobic biocathode communities. These bacteria are likely responsible for the oxygen reduction activity, given their low abundance in non-polarised control communities, and should be a target for isolation and further characterization as part of future work. Microbial fuel cell polarisations have been conducted using both a bioanode and aerobic biocathode. The results from MFCs show a 9-fold increase in power output with an aerobic biocathode (62 μW cm^{-2}), compared to an unmodified carbon felt cathode (7 μW cm^{-2}). This peak power output was comparable to the peak power output obtained from a Pt cathode (70 μW cm^{-2}). This indicates that the aerobic biocathode can provide a promising self-sustained, free to use, stable alternative to chemical catalysts for ORR in MFCs.

Acknowledgements

The authors thank EPSRC Supergen Biological Fuel Cells (EP/

H019480/1) for funding this project.

Appendix A. Supplementary material

Supplementary material related to this article can be found at http://dx.doi.org/10.1016/j.jpowsour.2016.05.055.

References

[1] Parliamentary Office of Science and Technology, Energy and Sewage (POST PN282), 2007.
[2] B.E. Logan, Nat. Rev. Microbiol. 7 (2009) 375–381.
[3] B.E. Logan, J.M. Regan, Environ. Sci. Technol. 40 (2006) 5172–5180.
[4] K.B. Liew, W.R.W. Daud, M. Ghasemi, J.X. Leong, S.S. Lim, M. Ismail, Int. J. Hydrogen Energy 39 (2014) 4870–4883.
[5] S. Freguia, K. Rabaey, Z. Yuan, J. Keller, Electrochim. Acta 53 (2007) 598–603.
[6] B. Erable, N. Duteanu, S.M.S. Kumar, Y. Feng, M.M. Ghangrekar, K. Scott, Electrochem. Commun. 11 (2009) 1547–1549.
[7] F. Zhao, F. Harnisch, U. Schröder, F. Scholz, P. Bogdanoff, I. Herrmann, Electrochem. Commun. 7 (2005) 1405–1410.
[8] E. Yu, S. Cheng, K. Scott, B. Logan, J. Power Sources 171 (2007) 275–281.
[9] R. Burkitt, T.R. Whiffen, E.H. Yu, Appl. Catal. B Environ. 181 (2016) 279–288.
[10] F. Zhang, S. Cheng, D. Pant, G. Van Bogaert, B.E. Logan, Electrochem. Commun. 11 (2009) 2177–2179.
[11] H. Rismani-Yazdi, S.M. Carver, A.D. Christy, O.H. Tuovinen, J. Power Sources 180 (2008) 683–694.
[12] F. Zhang, D. Pant, B.E. Logan, Biosens. Bioelectron. 30 (2011) 49–55.
[13] P. Clauwaert, D. Van der Ha, N. Boon, K. Verbeken, M. Verhaege, K. Rabaey, W. Verstraete, Environ. Sci. Technol. 41 (2007) 7564–7569.
[14] Y. Du, Y. Feng, Y. Dong, Y. Qu, J. Liu, X. Zhou, N. Ren, RSC Adv. 4 (2014) 34350–34355.
[15] Z. Wang, Y. Zheng, Y. Xiao, S. Wu, Y. Wu, Z. Yang, F. Zhao, Bioresour. Technol. 144 (2013) 74–79.
[16] G.-D. Zhang, Q.-L. Zhao, Y. Jiao, J.-N. Zhang, J.-Q. Jiang, N. Ren, B.H. Kim, J. Power Sources 196 (2011) 6036–6041.
[17] G.-W. Chen, S.-J. Choi, T.-H. Lee, G.-Y. Lee, J.-H. Cha, C.-W. Kim, Appl. Microbiol. Biotechnol. 79 (2008) 379–388.
[18] K. Rabaey, S.T. Read, P. Clauwaert, S. Freguia, P.L. Bond, L.L. Blackall, J. Keller, ISME J. 2 (2008) 519–527.
[19] H. Wang, S.C. Jiang, Y. Wang, B. Xiao, Bioresour. Technol. 138 (2013) 109–116.
[20] Y. Sun, J. Wei, P. Liang, X. Huang, AMB Expr. 2 (2012) 1–8.
[21] G. Zhang, Q. Zhao, Y. Jiao, K. Wang, D.-J. Lee, N. Ren, Biosens. Bioelectron. 31 (2012) 537–543.
[22] M. Rothballer, M. Picot, T. Sieper, J.B.A. Arends, M. Schmid, A. Hartmann, N. Boon, C.J.N. Buisman, F. Barrière, D.P. Strik, Bioelectrochemistry 106 (2015) 167–176.
[23] K. Chung, I. Fujiki, S. Okabe, Bioresour. Technol. 102 (2011) 355–360.
[24] C. Reimers, P. Girguis, H. Stecher, L. Tender, N. Ryckelynck, P. Whaling, Geobiology 4 (2006) 123–136.
[25] L. De Schamphelaire, P. Boeckx, W. Verstraete, Appl. Microbiol. Biotechnol. 87 (2010) 1675–1687.
[26] S.M. Strycharz-Glaven, R.H. Glaven, Z. Wang, J. Zhou, G.J. Vora, L.M. Tender, Appl. Environ. Microbiol. 79 (2013) 3933–3942.
[27] Z. Wang, D.H. Leary, A.P. Malanoski, R.W. Li, W.J. Hervey, B.J. Eddie, G.S. Tender, S.G. Yanosky, G.J. Vora, L.M. Tender, Appl. Environ. Microbiol. 81 (2015) 699–712.
[28] G.-W. Chen, S.-J. Choi, J.-H. Cha, T.-H. Lee, C.-W. Kim, Korean J. Chem. Eng. 27 (2010) 1513–1520.
[29] X. Xia, Y. Sun, P. Liang, X. Huang, Bioresour. Technol. 120C (2012) 26–33.
[30] M. Rimboud, E. Desmond-Le Quemener, B. Erable, T. Bouchez, A. Bergel, Bioelectrochemistry 102 (2015) 42–49.
[31] E. Blanchet, S. Pécastaings, B. Erable, C. Roques, A. Bergel, Bioresour. Technol. 173 (2014) 224–230.
[32] B. Erable, D. Féron, A. Bergel, ChemSusChem 5 (2012) 975–987.
[33] M. Rosenbaum, F. Aulenta, M. Villano, L.T. Angenent, Bioresour. Technol. 102 (2011) 324–333.
[34] A. Ter Heijne, O. Schaetzle, S. Gimenez, F. Fabregat-Santiago, J. Bisquert, D.P.B.T.B. Strik, F. Barriere, C.J.N. Buisman, H.V.M. Hamelers, Energy Environ. Sci. 4 (2011) 5035–5043.
[35] A. Ter Heijne, D.P.B.T.B. Strik, H.V.M. Hamelers, C.J.N. Buisman, Environ. Sci. Technol. 44 (2010) 7151–7156.
[36] D.B. Freitas, M.P. Reis, L.M. Freitas, P.S. Assis, E. Chartone-Souza, A.M. Nascimento, Can. J. Microbiol. 54 (2008) 996–1005.
[37] A. ter Heijne, H.V.M. Hamelers, M. Saakes, C.J.N. Buisman, Electrochim. Acta 53 (2008) 5697–5703.
[38] A. ter Heijne, H.V.M. Hamelers, C.J.N. Buisman, Environ. Sci. Technol. 41 (2007) 4130–4134.
[39] T. Zhang, M.-F. Shao, L. Ye, ISME J. 6 (2012) 1137–1147.
[40] J.G. Caporaso, J. Kuczynski, J. Stombaugh, K. Bittinger, F.D. Bushman, E.K. Costello, N. Fierer, A.G. Pena, J.K. Goodrich, J.I. Gordon, Nat. Methods 7 (2010) 335–336.
[41] M.N. Price, P.S. Dehal, A.P. Arkin, Mol. Biol. Evol. 26 (2009) 1641–1650.
[42] S. Cheng, H. Liu, B.E. Logan, Environ. Sci. Technol. 40 (2006) 364–369.
[43] A. Kleinhofs, W.M. Owais, R.A. Nilan, Mutat. Res. Rev. Genet. Toxicol. 55 (1978) 165–195.
[44] M.L. Snyder, H.C. Lichstein, J. Infect. Dis. 67 (1940) 113–115.
[45] H.C. Lichstein, M.H. Soule, J. Bacteriol. 47 (1944) 221.
[46] P.S. Bonanni, G.D. Schrott, L. Robuschi, J.P. Busalmen, Energy Environ. Sci. 5 (2012) 6188–6195.
[47] N.S. Malvankar, D.R. Lovley, ChemSusChem 5 (2012) 1039–1046.
[48] S. Freguia, S. Tsujimura, K. Kano, Electrochim. Acta 55 (2010) 813–818.
[49] L.M. Prescott, J.P. Harley, D.A. Klein, Int. Microbiol. (2002) 234.
[50] X. Zhu, M.D. Yates, B.E. Logan, Electrochem. Commun. 22 (2012) 116–119.
[51] B. Erable, I. Vandecandelaere, M. Faimali, M.-L. Delia, L. Etcheverry, P. Vandamme, A. Bergel, Bioelectrochemistry 78 (2010) 51–56.
[52] A. Cournet, M.-L. Délia, A. Bergel, C. Roques, M. Bergé, Electrochem. Commun. 12 (2010) 505–508.
[53] S. Parot, I. Vandecandelaere, A. Cournet, M.-L. Délia, P. Vandamme, M. Bergé, C. Roques, A. Bergel, Bioresour. Technol. 102 (2011) 304–311.
[54] S. Debuy, S. Pecastaings, A. Bergel, B. Erable, Int. Biodeterior. Biodegrad. 103 (2015) 16–22.
[55] K. Wetser, E. Sudirjo, C.J. Buisman, D.P. Strik, Appl. Energy 137 (2015) 151–157.
[56] P. Cristiani, M. Carvalho, E. Guerrini, M. Daghio, C. Santoro, B. Li, Bioelectrochemistry 92 (2013) 6–13.
[57] L. Malaeb, K.P. Katuri, B.E. Logan, H. Maab, S. Nunes, P.E. Saikaly, Environ. Sci. Technol. 47 (2013) 11821–11828.